Effect of active chilled beam layouts on ventilation performance and thermal comfort under variable heat gain conditions

Ming, R. ORCID: https://orcid.org/0000-0003-3703-600X, Mustakallio, P. ORCID: https://orcid.org/0000-0002-9042-8240, Kosonen, R., Kaukola, T., Kilpeläinen, S. ORCID: https://orcid.org/0000-0001-6218-187X, Li, B., Wu, Y. and Yao, R. ORCID: https://orcid.org/0000-0003-4269-7224 (2023) Effect of active chilled beam layouts on ventilation performance and thermal comfort under variable heat gain conditions. Building and Environment, 228. 109872. ISSN 1873-684X doi: 10.1016/j.buildenv.2022.109872 Available at https://centaur.reading.ac.uk/110001/

Effect of active chilled beam layouts on ventilation performance and thermal comfort under variable heat gain conditions

Ru Ming [a,b], Panu Mustakallio [c,d], Risto Kosonen [d,e], Tuomas Kaukola [c], Simo Kilpeläinen [d], Baizhan Li [a,b], Yuxin Wu [f], Runming Yao [a,b,g,*]

a Joint International Research Laboratory of Green Buildings and Built Environments (Ministry of Education), Chongqing University, Chongqing 400045, China

b National Centre for International Research of Low-carbon and Green Buildings (Ministry of Science and Technology), Chongqing University, Chongqing 400045, China

c Halton Oy, Finland

d Department of Mechanical Engineering, Aalto University, Espoo, 02150, Finland

e College of Urban Construction, Nanjing Tech University, Nanjing, China

f School of Civil Engineering and Architecture, Zhejiang Sci-Tech University, Hangzhou, 310018, China

g School of the Built Environment, University of Reading, Reading RG6 6DB, UK

* Corresponding author. Joint International Research Laboratory of Green Buildings and Built Environments, Ministry of Education, Chongqing University, 400045, China.
E-mail address: r.yao@cqu.edu.cn

Abstract:

The active chilled beam system has been popularly used in office and meeting rooms. There are very few studies of their terminal configuration on the thermal comfort and ventilation performance of systems with different heat gains. A comparative experimental study was implemented in mock-up office and meeting rooms to provide a comprehensive evaluation of the airflow patterns, air distribution, ventilation effectiveness, and local thermal comfort of the 4-way system. Four different terminal layouts with two types of the chilled beams (600 unit and 1200 unit sized 0.6m x 0.6m and 1.2m x 0.6m, respectively) were tested at three heat gain levels: low (46W/m^2) and medium (66W/m^2) heat gains in the office room, and high (92W/m^2) heat gain in the meeting room. The results revealed that the terminal layouts and heat gain levels had significant effects on air distribution and local thermal comfort. The increased heat gains generated lower heat removal effectiveness, worse indoor thermal uniformity, and increased risk of draught. Generally, the 1200-unit system performed better than that with 600 units for heat removal effectiveness and contaminant removal effectiveness. In terms of local thermal comfort, the 600-unit system generally provided higher performance than that with the 1200-unit system. The practical recommendations for the system design and operation stages are provided based on the operating range of the 4-way systems under variable terminal layouts and heat gain conditions.

Keywords: 4-way active chilled beam system, thermal comfort, air distribution, terminal layout, heat gain level

1. Introduction

According to the World Health Organization (WHO), Coronavirus Disease 2019 (COVID-19) is

responsible for a cumulative death toll of 6.27 million worldwide as of May 20, 2022 [1]. Airborne transmission is the major route for the spread of COVID-19 pathogens [2]. With the outbreak of COVID-19, indoor ventilation effectiveness is receiving a growing amount of attention [3, 4]. Air distribution is essential for meeting the ventilation and thermal requirements of indoor spaces [5, 6], and an effective ventilation system design is a key factor in maintaining human thermal comfort and lowering the risk of airborne transmission [7-9].

The development of cutting-edge technologies has been a critical part of responding to and overcoming global issues [10]. Regarded as one of the most promising HVAC-related technologies by the American Council for Energy-Efficient Economy (ACEEE), the active chilled beam system becomes an alternative to traditional room ventilation and cooling systems and has been increasingly used in North America and Europe over the last two decades [11, 12]. The active chilled beam system is an air–water ACMV system which utilize primary and induced air as supply air [10]. The active chilled beams consist of fin-and-tube heat exchangers which induce air from the room. Primary air is forced through a set of nozzles from the Air Handling Unit (AHU), and a mixture of primary air and induced air (or secondary air) in the mixing chamber is supplied into the occupied zone as supply air [13]. The active chilled beams are typically fixed in the ceiling to achieve proper air distribution via the Coandă effect [14]. It is proven that the active chilled beam systems can reduce energy consumption by 30% in comparison to conventional HVAC systems [10].

There can be variations in airflow patterns and ventilation performance for different air distribution methods. Numerous studies have concentrated on comparing active chilled beam systems and other air distribution systems, including the conventional fan coil unit (FCU) system [12], the conventional overhead mixing ventilation system [15], the underfloor air distribution

(UFAD) system [15], and the chilled beam with radiant panel (CBR) system [16, 17]. The existing studies amply confirmed that the active chilled beam system could provide good air distribution patterns and cooling capacity [14, 18-20], energy-saving potential [21-24], and high-level comfort [12, 15, 25]. However, there is no denying that the performance of the active chilled beam systems also depends on the characteristics of the specific building and local climate [10].

To meet the requirement for airflow distribution in an indoor environment with the non-uniformity of heat gain distribution, active chilled beam systems can be classified into 1-way, 2-way, and 4-way systems according to the structural design [10]. Generally, a 1-way system is used in customized applications, such as in hospital patient rooms, where maintaining local indoor air quality and thermal comfort is highly important [26]. A majority of the existing experimental and simulation studies have aimed to provide design guidelines by evaluating the ventilation and comfort performance of 2-way active chilled beams as terminal units [14, 27-31]. Providing efficient mixing with the room air by creating multi-directional or circular air distribution patterns, has proven to be a dominant advantage of the 4-way active chilled beam system [25]. Despite these valuable contributions to the understanding of 1-way and 2-way systems, there is a lack of detailed information about the ventilation and comfort performance of 4-way systems.

The airflow pattern in the occupied zone is driven by a variety of factors, such as the level of internal heat gain [32], the location of heat gain [33], and the type [27] and symmetry [34] of the terminal units. It is worth mentioning that local thermal discomfort issues and energy consumption risks may still arise in 4-way active chilled beam systems because of improper installation. In particular, it was observed that maintaining a constant heat gain level during system operation is very challenging due to multiple variations in personnel and room functions. However, the existing

research does not shed light on the effect of different heat gain levels and different types/numbers of chilled beams on both thermal comfort and ventilation efficiency, with experimental studies especially lacking.

To fill the gap, this research is devoted to comprehensively evaluating the impact of the terminal layouts of the 4-way active chilled beam ventilation system on ventilation performance and local thermal comfort under variable heat gain conditions in mock-up office and meeting rooms. The research in this paper sets out to solve the following detailed questions on the performance of the 4-way active chilled beam system: 1) what is the effect of three heat gain levels (46W/m^2, 66W/m^2, and 92W/m^2)? and 2), what is the influence of different terminal layouts and types (600 units and 1200 units)? This comparative experimental study could be the first comprehensive evaluation of ventilation and comfort performance of the 4-way active chilled beam system and is critical to providing practical insights into the operating range of these systems under variable heat gain conditions.

2. Method

2.1. Test chamber and the 4-way active chilled beam design

To investigate the thermal and ventilation performance of the 4-way active chilled beam system, the experiments were conducted in a full-scale climate chamber designed to simulate office or meeting rooms, as shown in Fig.1. The chamber is located at the Kausala factory of the Oy Halton Group Ltd in Finland, with dimensions of 6.1m x 4.4m x 2.7m (L x W x H). Since the chamber is nested within a room, the lightweight wall constructed with MDF panels is regarded as the door side wall, and the length of the chamber was reduced from 6.5m to 6.1m. Therefore, the envelope of the

chamber was finished with a door side wall, a mock-up window wall, a side wall, and a thermally insulated observation window wall. Plywood construction and thermal insulation was installed on the walls, floors, and suspended ceiling of the chamber to avoid the effects of cold radiation. The external environment was maintained at approximately the same temperature as the average air temperature in the chamber. The two types of chilled beam devices were incorporated into the suspended ceiling. All the experiments were conducted under steady-state room conditions of 25°C indoor air temperature.

The active chilled beam devices with 4-way air distribution were applied to the test space. The operating principle of the device is shown in Fig.2(a). It consisted of a front panel, nozzles, plenum, brackets, spigot, frame, connection pipes, coil/heat exchanger, and integrated VAV supply air valve with motorized actuator. The primary supply air enters the plenum of the 4-way active chilled beam, from which it is diffused into the room through the nozzles and integrated VAV supply air valve, and then through supply slots. The air jets from the nozzles induce ambient room air efficiently through the heat exchanger, where the air is cooled by means of the cool water circulating in the heat exchanger. The supply slots direct the air jets horizontally along the ceiling surface. The indoor climate is controlled with Variable Air Volume (VAV) dampers and the active chilled beams' ventilation system with integrated supply air VAV function. These are used to adjust the ventilation airflow, room temperature, and indoor air quality in office spaces. In this study, two sizes of chilled beam were used: the 600 chilled beam sized 0.6m x 0.6m and the 1200 chilled beam sized 1.2m x 0.6m. The installation positions of the two types of chilled beam are shown in Fig.2(b).

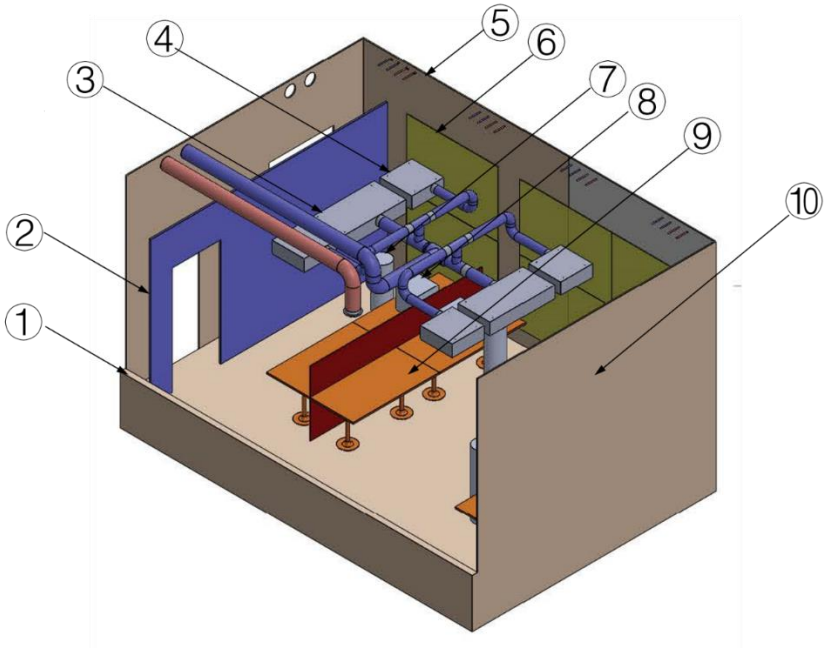

Fig. 1: Layout of the test chamber: ① observation window wall, ② door side wall, ③ 1200 chilled beam, ④ 600 chilled beam, ⑤ mock-up window wall, ⑥ electrical heating foil, ⑦ dummy (manikin), ⑧ computer, ⑨ table, ⑩ side wall.

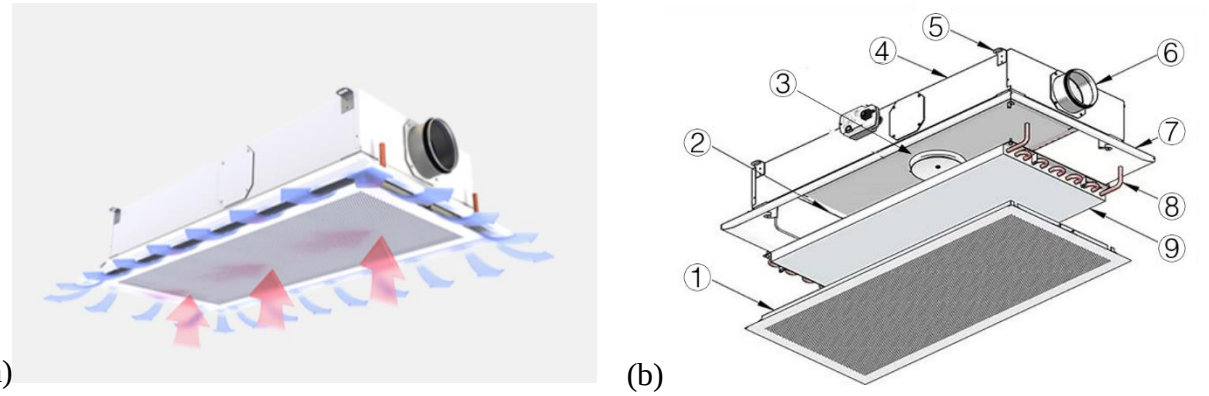

(a) (b)

Fig. 2: The 4-way active chilled beam system design, (a) air flows, where the red arrow shows the induced room air and the blue arrow is the total supply air; (b) structural design: ① front panel, ② nozzles, ③ integrated VAV supply air valve with motorized actuator, ④ plenum, ⑤ brackets, ⑥ spigot, ⑦ frame, ⑧ connection pipes, ⑨ coil/heat exchanger.

2.2. Experimental methods and instruments

Multichannel, low-velocity, omni-directional, thermistor anemometers (measurement system HT-400, manufactured by "Sensor") were used to measure the air temperature and velocity

distribution of the whole room, as shown in Fig.3. A set of omni-directional velocity probes (HT412) was used to measure air velocity and turbulent intensity. The accuracy and range of air velocity measurements is shown in Table 1. Air temperature measurements were carried out with PT100 sensor attachments near the velocity probes. To measure the distributions of air temperature and air velocity at different heights, six heights (0.1m, 0.6m, 1.1m, 1.7m, 2.2m, and 2.6m) were selected to represent distributions at the ankle level, the abdomen level, the sedentary breathing zone level, the standing breathing zone level, and the upper part of the room, respectively.

Supply and exhaust air temperatures were also measured by PT100 sensors. The supply and exhaust airflow measurements were carried out with orifice plates connected to FCO33 differential pressure transmitters. A Mikor TT470S micro-manometer was used to measure the air pressure difference in the duct prior to the chilled beam. In order to measure the indoor globe (operative) temperature, PT100 sensors were installed at the reference point located 0.8m above the floor in the middle of the room (see Fig.4).

A photoacoustic gas analyzer (Gasera One) was used to measure Sulfur Hexafluoride (SF_6) concentration. For each point, the sampling interval was 1 minute, and the samples were taken continuously over a period of 180 minutes.

The locations of measurement sampling points, the heat sources, the active chilled beams, and the exhaust are shown in Fig. 4. For the thermal environment measurements, there were altogether 42 grid locations in the office room and 44 grid locations in the meeting room. The test points and the heat sources for the dummy in both office and meeting settings were in close proximity at about 0.2m separation, which ensures that the measured temperature results are not influenced by the heat sources from the dummy.

Table 1: Ranges and accuracy of the measuring instruments.

Equipment	Variables	Range	Accuracy
Sensor/HT412	Air velocity	0.05 to 1.00m/s	±0.02m/s
Sensor/PT100	Air, globe and water temperature	−50 to 100°C	±0.2°C
Furness Controls/FCO33	Airflow rate	/	5% of reading
Mikor/TT470S	Air pressure	0–199.9Pa	±0.6Pa
Krohne Electromagnetic flow meter IFC 010	Water flow rate	/	0.5% of reading
Multipoint meter/ Gasera One	SF_6 concentration	/	< ± (50ppm + 2% of measuring value)

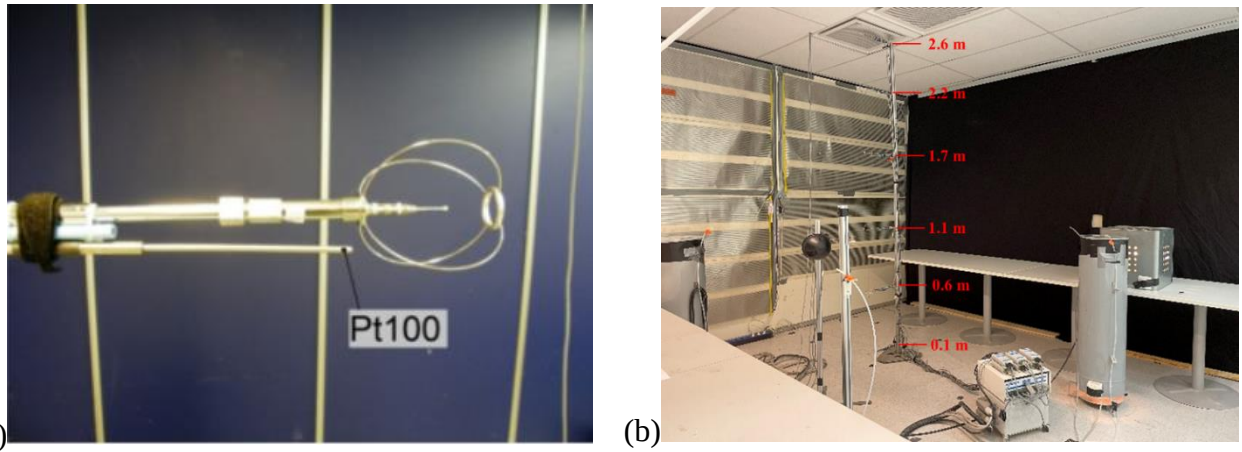

(a) (b)

Fig. 3: (a) The air velocity probe (HT412) and air temperature sensor (Pt100); (b) the heights of the sensors.

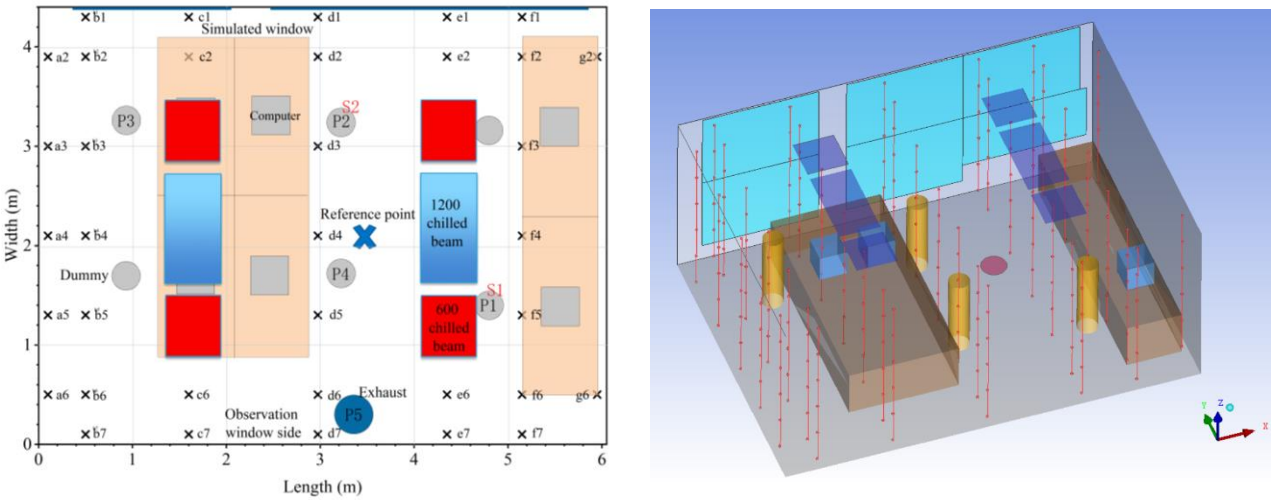

(a) Office room

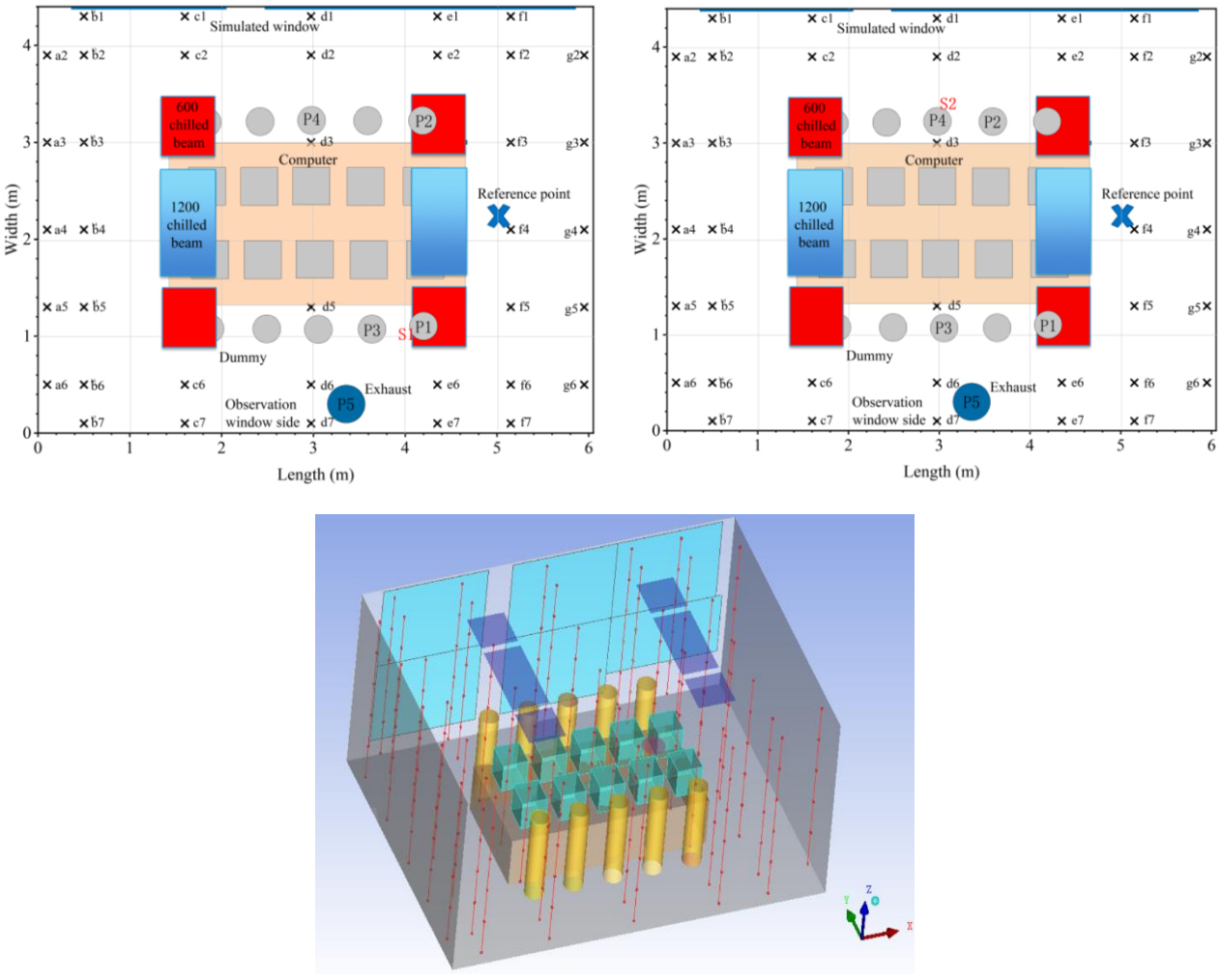

(b) Meeting room

Fig. 4: The locations of sampling points, where a2 to g6 represent the thermal environment sampling points, P1 to P4 represent the locations of pollutant sampling points, S1 to S2 represent the pollutant sources, and the red lines with six red points represent the sampling points at six heights.

2.3. Studied cases

Three heat gain levels and two types of chilled beam were adopted to analyze the effect of the different heat gain levels and different types of chilled beam on air distribution and thermal comfort. As shown in Table 2, the three heat gain levels were 46W/m^2, 66W/m^2, and 92W/m^2, representing the low, medium, and high levels, respectively. These office and meeting room cases represent typical new European office buildings. Office layout and simulated window sizes are based on one real office building in Helsinki. The people density and heat load levels represent typical levels in different occupancy/layout situation. To represent a seated occupant, a cylindrical dummy of 1.2m height and 0.3m diameter was used, with light bulbs inside to simulate the heat of 75W for each human body. Likewise, the mock-up computer (0.4x0.4x0.4m) was made of an iron sheet containing light bulbs and the heat gain of one mock-up computer was 100W.

As a result of adjusting the number of mock-up occupants and computers, three levels of indoor heat gain were obtained. For all cases, the heat gain from the lighting was 112W and the mock-up solar heat gain was 600W. For the low heat gain conditions, three mock-up occupants (3 x 75W) and three computers (3*100W) were arranged in the office room along with three tables (1600x 800mm). For the medium heat gain conditions, six mock-up occupants (6x75W) and six computers (6x100W) were arranged in the office room with six tables (1600x800mm). For the high heat gain conditions, ten mock-up occupants (10x75W) and ten computers (10x100W) were arranged in the meeting room, with a one table (3200x1600mm) in the middle. There were four different terminal layouts of the

4-way active chilled beam system in the low heat gain conditions, including 4 pcs of 600 chilled beam, 2 pcs of 600 chilled beam, 2 pcs of 1200 chilled beam, and 1 pc of 1200 chilled beam. There were two types of terminal layouts under the medium and high heat gain conditions, included 4 pcs of 600 chilled beam and 2 pcs of 1200 chilled beam. In order to maintain the room temperature at 25°C in all cases, the supply airflow rate was accordingly 2.4 ACH[1] (1.8 l/s,m^2_{floor}), 4.2 ACH (3.2 l/s,m^2_{floor}), and 5.8 ACH (4.3 l/s,m^2_{floor}).

[1] ACH: air change rate per hour

Table 2: Measuring the heat gains and cooling powers of water and air in chilled beams.

Case	Room type	Chilled Beam (number and types)	Heat gain (W)					(W/m^2)	Supply airflow rate		ACH	Cooling from air side	Water cooling
			Occupant	Computer	Lighting	Solar	Total	per m^2	L/s	L/(s·m^2)	h^{-1}	W	W
O-Low-4x600	Office	4 pcs 600	3×75	3×100	112	600	1237	46	48	1.8	2.4	518	719
O-Low-2x600	Office	2 pcs 600											
O-Low-2x1200	Office	2 pcs 1200											
O-Low-1x1200	Office	1 pc 1200											
O-Medium-4x600	Office	4 pcs 600	6×75	6×100	112	600	1762	66	84	3.2	4.2	907	855
O-Medium-2x1200	Office	2 pcs 1200											
M-High-4x600	Meeting	4 pcs 600	10×75	10×100	112	600	2462	92	115	4.3	5.8	1242	1220
M-High-2x1200	Meeting	2 pcs 1200											

2.4. Experimental procedure

The experimental procedures involved smoke visualization experiments, environmental parameter tests, and concentration measurements. Prior to the measurements, all the measuring equipment was calibrated and sufficient time was provided in each measurement step to ensure that all the measurements were carried out in steady-state conditions.

Firstly, the airflow patterns of the eight ventilation systems were observed by smoke visualization experiments. A portable fog generator (Martin Magnum 850, UK) introduced smoke into the room by way of the supply inlet, and the path of the supply airflow could be visualized and captured with a digital camera (GoPro Hero7, USA). To capture the whole process of airflow patterns, the visualization experiment in each case took about 120min.

Secondly, the indoor air temperature and air velocity measurements were carried out in the office and meeting rooms (see Fig. 4). The sampling rate for air temperature and air velocity measurements was 5 times/s and the sampling interval for these measurements was 3 minutes. So the readings were the average values of 3 minutes. In addition, at least 5 minutes between adjacent tests was required so that the data would represent steady-state conditions. Since it is impractical to measure the entire space simultaneously, the indoor air temperature and air velocity measurements were conducted sampling point by sampling point, which lasted about 360 min in each case.

Tracer gas concentrations were measured at sampling points *P1*, *P2*, *P3*, *P4*, and *exhaust*, as shown in Fig.4. The measuring height of each sampling point was 1.1m above the floor. A multipoint meter (Gasera One) was used to measure the concentration of pollutants at different points simultaneously. Two sources (*S1* and *S2*) were set up in the office and the meeting room. When the pollution source is at point S1, then P1 is the closest measurement point to the pollution source. If the

source of the pollution is located at S2, P2 and P4 represent the measuring points near the pollution source in the office and meeting room, respectively. The tracer gas used in this study was SF_6 to evaluate the ventilation effectiveness of the eight chilled beam systems when the room concentrations were maintained constant. Tracer gas is released at a rate of 2ml/s and the sampling frequency was 1 min. The measuring duration of the concentration of SF_6 during each case was 180min to allow the concentration of tracer gas in the room air to reach a steady state.

2.5. Evaluation indices

Performance of the 4-way active chilled beam systems regarding ventilation efficiency and thermal comfort for the occupied zone was analyzed.

Contaminant removal effectiveness (CRE) was proposed to measure the ability of air distributions to remove contaminants [35], as follows:

$$\varepsilon = \frac{C_e - C_s}{C_i - C_s} \quad (1)$$

where ε is the contaminant removal effectiveness; C_e is the concentration of contaminant at the exhaust; C_s is the concentration of contaminant of the supply air; C_i is the concentration of contaminant of the test point. In a fully mixed room, the CRE is equal to 1. The higher the contaminant removal effectiveness, the better is the air distribution system's ability to remove contaminants, and therefore the indoor air quality is higher.

Heat removal efficiency (HRE) indicates the ability to remove heat from a space:

$$\mathrm{HRE} = \frac{T_e - T_s}{T_{avg(1.1-0.1)} - T_s} \quad (2)$$

where T_e is the temperature at the exhaust terminal, °C; T_s is the supply air temperature in °C;

$T_{avg(1.0-0.1)}$ indicates the average air temperature at heights of 0.1m to 1.1m.

The vertical air temperature difference (VATD) between head and ankles results in occupants' local thermal discomfort [36-39], so we examined the vertical air temperature for sedentary ($\Delta T_{1.1-0.1}$) and standing ($\Delta T_{1.7-0.1}$) occupants:

$$\Delta T_{1.1-0.1} = T_{1.1} - T_{0.1} \tag{3}$$

$$\Delta T_{1.7-0.1} = T_{1.7} - T_{0.1} \tag{4}$$

where $T_{0.1}$ is the air temperature (°C) at a height of 0.1m in the occupied zone; $T_{1.1}$ is the air temperature (°C) at a height of 1.1m in the occupied zone; $T_{1.7}$ is the air temperature (°C) at a height of 1.7m in the occupied zone.

The local thermal discomfort was also evaluated by the draught rate index. A draught rate model was developed by Fanger and Christensen to predict the percentage of unwanted local cooling of a human body part caused by air movements [40]. The draught rate was calculated by Eq.(5):

$$DR = (34 - T_a)(v - 0.05)^{0.62}(0.37vTu + 3.14) \tag{5}$$

where T_a is the local air temperature (°C); v is the local air velocity, m/s; and Tu is the local turbulence intensity, %.

Turbulence intensity (Tu) is defined by the following equation:

$$Tu = \frac{v'}{v} \times 100\% \tag{6}$$

where v' is the standard deviation of the velocity fluctuation.

The effective draft temperature (EDT) is defined by Eq. (7), as:

$$EDT = \left(T_a - T_{avg}\right) - 8\left(v - v_{avg}\right) \tag{7}$$

where T_a is local air temperature (°C); T_{avg} is average room temperature (°C); v is local air velocity, m/s; and v_{avg} is average room air velocity, m/s. EDT values that are lower indicate a more

uniform interior thermal environment.

The air diffusion performance index (ADPI) is used to describe the air distribution performance of an air distribution device, measuring the uniform distribution of temperature and air velocity within an occupied area [41]. Additionally, ADPI is one way to rate the uniformity of a given thermal environment, which is closely linked to thermal comfort. As described in the following equations, ADPI can be defined as the percentage of points in a room that are within both the effective draught temperature and velocity range for a comfortable climate [15]:

$$-1.5\ ^{\circ}\mathrm{C} < T_{ed} < +1.0\ ^{\circ}\mathrm{C}\ and\ v < 0.35\ m/s \tag{8}$$

$$\mathrm{T}_{ed} = \left(T - T_{avg}\right) - 7.73(v - 0.15) \tag{9}$$

3. Results and analysis

3.1. Visualization of airflow patterns

By performing the smoke tests, the prevailing airflow patterns have been captured to provide an indication of the airflow characteristics of the active chilled beam system with different heat gains and different chilled beam types. To convey the airflow pattern clearly, the visualization of airflow patterns was implemented in the width direction of the room (Y axis in Fig.4). Fig.5 demonstrates a clear process of the 4-way active chilled beam system whereby the airflow stayed attached to the ceiling instead of falling directly into the occupied area.

Under the low heat gain conditions, the air jet is attached to the ceiling and moves in a horizontal direction. In the O-Low-4×600 case, the air released from the four chilled beams moved first along the ceiling, then the supply air from both chilled beams was merged near the observation window side because of the convection flow of the mock-up window. After that, the two air streams

detached from the ceiling and moved downward along the observation window together. Compared to the 4 pcs of 600 chilled beam case, the cool supply air in the case with 2 pcs of 600 chilled beam diffused across a wider range horizontally at the ceiling due to the lack of any disturbance of the supply air from the opposite beam. That was also caused by the greater momentum of the supply air jets from two chilled beams instead of the same total supply airflow rate from four. With the assistance of the thermal plume created by the heat source, cool supply air in the O-Low-2×1200 case and the O-Low-1×1200 case retarded the process of moving downward when it met the convection flow of the heat source, and afterward the supply air jet turned directly at the head-chest zone. In that situation, there is also a risk of draught.

Both the O-Low-4 × 600 case and O-Medium-4 × 600 case had a similar air diffusion performance, but due to buoyancy, the airflow in the O-Medium-4×600 case rose before descending to the floor. For the high heat gain conditions, a thermal plume generated by a heat source, like a computer, allowed the cool supply air to rise upward, so the cold air diffused and mixed above the occupied area. Under the medium and high heat gain conditions, the increase in heat gain dramatically altered the airflow pattern, resulting in the jet turning directly to the occupied zone and having an adverse effect on local thermal comfort.

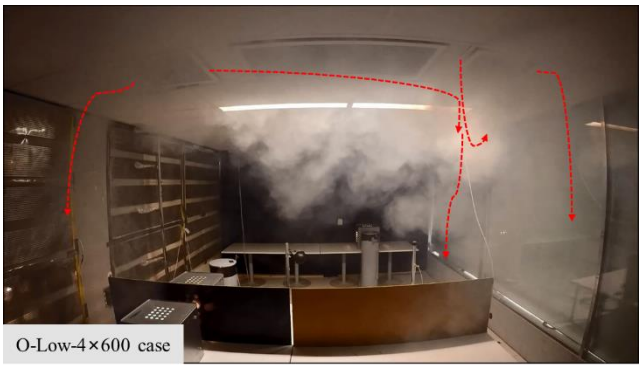
O-Low-4×600 case

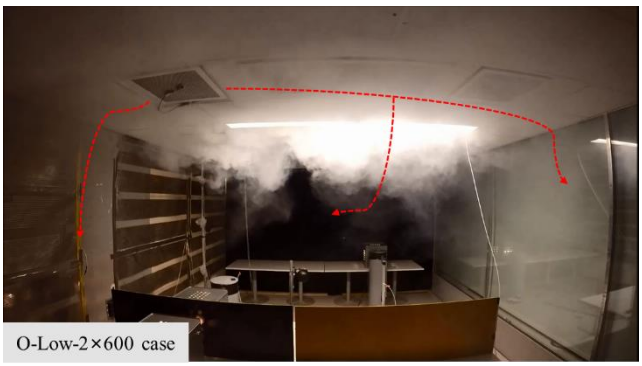
O-Low-2×600 case

Fig. 5: The visualized airflow patterns under different heat gains and different chilled beam types. (Note: Red arrows depict the direction of the supply air in those conditions.)

3.2. Characteristics of the airflow distribution

To assess the airflow distribution of the 4-way active chilled beam system, the distribution of the air velocity in the occupied zone under different heat gains is illustrated in Figs.6 and 7. It can be seen from Fig.6 that for the low heat gain conditions, the air velocity in the occupied zone had a range of 0.05m/s to 0.25m/s and the mean value of the four low heat gain cases was around 0.11m/s. The distribution of air velocity was very similar between the 4 pcs of 600 chilled beam system and the 2 pcs of 600 chilled beam system, and focused primarily on the lower air velocity values. It

demonstrated that in low heat gain conditions, the thermal environment could be adjusted by using two or four units to provide a good and individually adjusted thermal environment. The proportion of higher air velocity distribution was higher in the 1 pc of 1200 chilled beam system than in the 2 pcs of 1200 chilled beam system, which indicated a uniform air velocity distribution in the O-Low-2× 1200 case.

To further explore the influence of various numbers and types of chilled beam systems, Fig.7 visualizes the air velocity in the center plane of the room under low heat gain conditions. For the O-Low-4 × 600 case, the inlet airflow was supplied horizontally along the ceiling and went downwards along the walls. A similar distribution of air velocity was achieved in the O-Low-2×600 case despite having two fewer chilled beams. Compared to the occupied zone, the upper area of the room had much higher air velocity. For the O-Low-2×1200 case, the air from the two pcs of chilled beam dispersed over a wider range, and the air velocity was higher at the edge of the upper area of the room. The airflow mixed above the occupied zone, and created a similar airflow distribution to the 4×600 case and 2×600 case in the occupied zone. With 1 pc of chilled beam, there was a higher air velocity along the left wall where the air-jet attached to the wall in the O-Low-1×1200 case, and this system had the most non-uniform indoor air velocity distribution. Therefore, the system with 2 pcs of 1200 units performed well under the low heat gain conditions, and was similar to the 4 pcs of 600 units. But two units' layout did not perform well if only one of these units was "activated".

For the medium heat gain conditions, Fig.6 illustrates that the air velocity in the occupied zone ranged from 0.05m/s to 0.29m/s with a mean value of 0.13m/s. Compared with the O-Medium-2× 1200 system, the O-Medium-4×600 system had a higher proportion of lower air velocity distribution, but simultaneously had a higher maximum value. The high heat gain conditions had a wide air

velocity range, and the mean value of air velocity of the M-High-4×600 and M-High-2×1200 systems were 0.15m/s and 0.16m/s, respectively. Overall, these results suggest that the range of air velocity distribution was expanded with an increase in the heat gains, and the majority of air velocities were between 0.05 and 0.2m/s for all cases. Compared with other types and numbers of chilled beams, the 1 pc of 1200 chilled beam system resulted in a more non-uniform and immoderate air distribution.

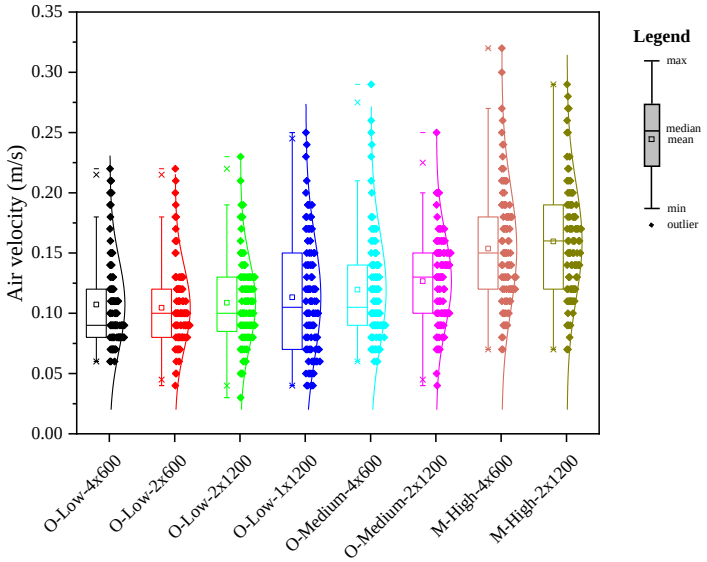

Fig. 6: The distribution of air velocity in the occupied zone with different chilled beam types.

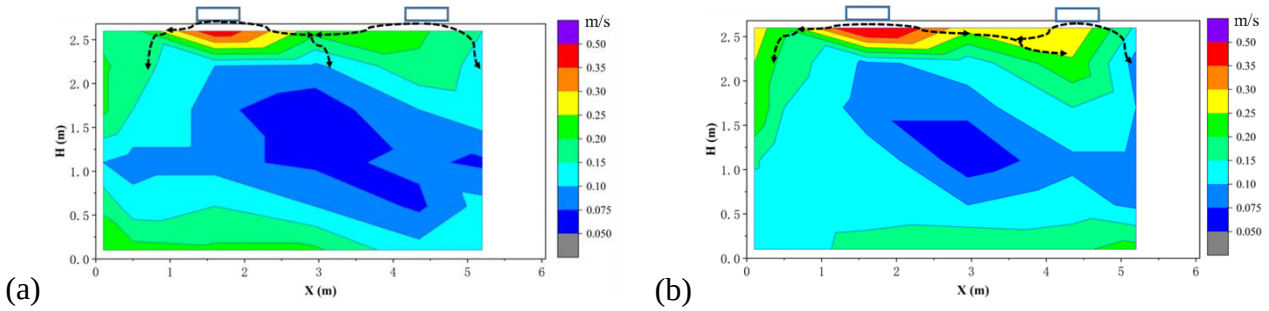

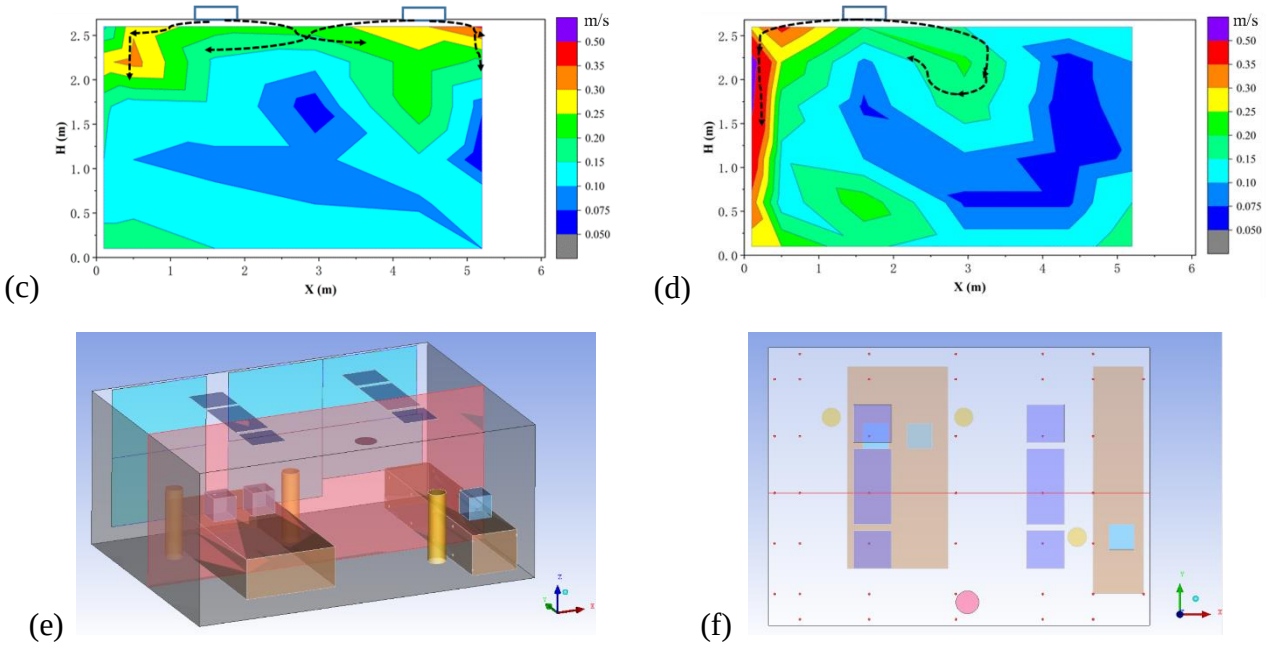

Fig.7: The contour plot of the air velocity in the plane below the central line of the low heat gain cases, (a) O-Low-4x600; (b) O-Low-2x600; (c) O-Low-2x1200; (d) O-Low-1x1200; (e) elevations of the test points; (f) plane of the test points.
(Note: The blue box at the top of the picture represents the terminal units, and the black arrows depict the direction of the supply air in those conditions.)

Fig.8 presents the distribution of air temperature in the occupied zone under different heat gains and different chilled beam types. For the low heat gain and medium heat gain conditions, the mean value of each case was around 24.3°C and ranged from 23.5°C to 25.2°C. For the two high heat gain cases, the air temperature distribution was more non-uniform and had a larger range of air temperature because of the high supply airflow rate and cooling power. The air temperature of the M-High-4×600 system ranged from 23.5°C to 25.8°C with a mean value of 24.4°C, while in the M-High-2×1200 case, it ranged from 24.0°C to 26.0°C with a mean value of 24.6°C.

To provide a more detailed understanding of the thermal environment achieved under each system, Table 3 summarizes the measurement results, including the air temperature, operative temperature, horizontal air temperature difference, and vertical air temperature difference at the occupied zone. The average temperature was similar in the eight studied cases, whether it was the

average air temperature or average operative temperature. Given the effect of the mean radiant temperature, the operative temperature was slightly higher than the air temperature at the reference point in all cases, and the difference was about 0.5°C. At the height of 1.1m, the horizontal air temperature difference between the mock-up window side and the observation window side under low, medium, and high heat gain conditions was 0.4°C, 0.5°C, and 0.7°C, respectively. Under the low heat gain conditions, the average air temperature on the door side was lower than that on the wall side. It is also noticed that the average air temperature on the door side was higher than the wall side in the O-Low-2×600 case, which was opposite to the other low heat gain cases. Under the medium gain conditions, the case with 4 pcs of 600 chilled beam and the case with 2 pcs of 1200 chilled beam displayed an opposite tendency. The M-High-2x1200 case exhibited a similar average temperature on both door and wall sides, indicating a more uniform environment in the horizontal direction. In addition, it was roughly the same scenario at a height of 0.1m as at a height of 1.1m.

Results for the air temperature shown in Table 3 also agreed with the smoke tests in Fig.4. The O-Low-1×1200 case displayed a big vertical temperature difference because there was a chilled beam only on the left side of the room, while the vertical temperature stratification on the right side was evident. For the M-High-4x600 case, the range of the vertical air temperature difference was the largest and the air temperature was highest in the area above the occupied zone, where the airflow was influenced by the dual function of the strong upward buoyancy caused by the thermal heat gain and the downward cold jet from the chilled beam.

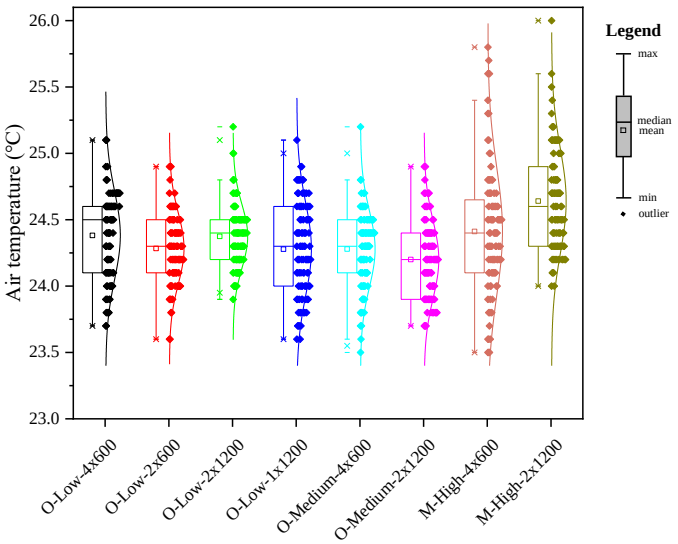

Fig.8: The distribution of air temperature in the occupied zone with different chilled beam types.

Table 3: Summary of measurement results in the occupied zone of different cases.

	The low heat gain case (46 W/m^2)				The medium heat gain case (66 W/m^2)		The high heat gain case (92 W/m^2)	
	O-Low-4x600	O-Low-2x600	O-Low-2x1200	O-Low-1x1200	O-Medium-4x600	O-Medium-2x1200	M-High-4x600	M-High-2x1200
Average air temperature [°C]	24.4	24.3	24.4	24.3	24.3	24.2	24.4	24.6
Max. [°C]	25.1	24.9	25.2	25.1	25.2	24.9	25.8	26.0
Min. [°C]	23.7	23.6	23.9	23.6	23.5	23.7	23.5	24.0
Std. dev. [°C]	0.3	0.3	0.2	0.3	0.3	0.3	0.5	0.4
Temperature at the reference point[2]:								
Operative temperature [°C]	25.3	25.1	25.2	25.4	25.3	25.1	24.9	25.1
Air temperature [°C]	24.8	24.5	24.7	24.9	24.7	24.4	24.5	24.7
Operative and air temp. diff. [°C]	0.5	0.6	0.6	0.5	0.5	0.6	0.4	0.4
Avg. air temperature at height 0.1 m:								
Mock-up window side [°C]	24.5	24.4	24.4	24.3	24.3	24.5	24.6	25.0

[2] The location of the reference point is shown in Fig. 4, which is at a height of 1.1m.

Observation window side [°C]	24.2	24.2	24.2	23.9	23.9	23.9	23.9	24.2
Avg. horizontal air temp. diff. [°C]	0.3	0.2	0.2	0.4	0.4	0.6	0.7	0.8
Door side [°C]	23.9	24.6	24.0	23.8	24.0	24.2	24.4	24.4
Wall side [°C]	24.6	23.8	24.6	24.1	24.3	23.9	23.9	24.4
Avg. horizontal air temp. diff. [°C]	-0.7	0.8	-0.6	-0.3	-0.3	0.3	0.5	0
Avg. air temperature at height 1.1 m:								
Mock-up window side [°C]	24.6	24.5	24.7	24.5	24.5	24.6	24.7	25.0
Observation window side [°C]	24.2	24.1	24.3	24.2	24.1	23.9	24.0	24.3
Avg. horizontal air temp. diff. [°C]	0.4	0.4	0.4	0.3	0.4	0.7	0.7	0.7
Door side [°C]	24.1	24.5	24.2	24.1	24.2	24.4	24.5	24.6
Wall side [°C]	24.8	24.1	24.6	24.5	24.5	24.1	24.2	24.5

Avg. horizontal air temp. diff. [°C]	-0.7	0.4	-0.4	-0.4	-0.3	0.3	0.3	0.1
At height 0.1 m – 1.1 m:								
Avg. vertical air temp. diff. [°C]	0.2	0.1	0.2	0.3	0.3	0.1	0.2	0.1
Max. vertical air temp. diff. [°C]	0.4	0.4	0.5	0.7	0.7	0.3	0.5	0.3
Min. vertical air temp. diff. [°C]	-0.1	-0.3	-0.1	0.0	0.0	-0.1	-0.5	-0.2
Std. dev. of vertical air temp. diff. [°C]	0.1	0.2	0.2	0.2	0.2	0.1	0.3	0.1
At height 0.1 m – 1.7 m:								
Avg. vertical air temp. diff. [°C]	0.2	0.1	0.1	0.5	0.3	0.2	0.3	0.2
Max. vertical air temp. diff. [°C]	0.6	0.4	0.4	0.9	0.9	0.4	1.5	0.5
Min. vertical air temp. diff. [°C]	-0.1	-0.3	-0.1	0.2	-0.1	-0.1	-0.5	-0.4
Std. dev. of	0.2	0.2	0.2	0.2	0.2	0.1	0.4	0.2

vertical air
temp. diff. [°C]

3.3. Ventilation effectiveness

To assess the ventilation effectiveness of the eight air distribution strategies, Table 4 presents the contaminant removal effectiveness (CRE) at different test points for each of the two pollutant source locations. The CRE at test points P1 to P4 is indicated by ε_{P1}, ε_{P2}, ε_{P3}, and ε_{P4} with ε_{mean} representing the mean value of CRE at the three measuring points other than the point close to the pollution source. When the source was located at point S1, P1 was the measuring point close to the pollution source; similarly, when the source was located at S2, P2 was the measuring point close to the pollution source in the office room and P4 in the meeting room (see Fig.4).

As shown in Table 4, there was no significant difference between the mean value of CRE for the different chilled beam systems. Overall, the active chilled beam systems under the low and medium heat gain conditions presented a better contaminant removal effectiveness than under the high heat gain conditions. For the low heat gain conditions, the O-Low-2x600 case achieved peak performance in removing contaminants. For the medium and high heat gain conditions, the 2 pcs of 1200 units displayed better contaminant removal effectiveness than the 4 pcs of 600 units.

There was a slight difference between different pollution source locations, reflecting the closeness of the mean CRE values for the two pollution source locations in the same case. This phenomenon was particularly pronounced in the O-Low-1x1200, O-Medium-4x600, and M-High-4x600 cases. For the O-Medium-4x600 case and the M-High-4x600 case, the difference between the two sources was the largest at 0.18 and 0.19 respectively.

In addition, it is worth noting that the chilled beam systems under low heat gain and medium heat gain conditions can remove the pollutants near the source effectively, while this effect was not obvious under the high heat gain conditions. With the source at point S1, P3 had the highest CRE

under the low and medium heat gain conditions since it was farthest from the pollution source. There was roughly the same distance from each measuring point to the pollution source when the pollution source was at point S2. P3 illustrated the best performance in removing the contaminants under the low heat gain conditions and P1 showed the best performance under the medium heat gain conditions. Under the high heat gain conditions, a complex local airflow pattern led to a non-uniform dispersion of contaminants and resulted in poor performance near the source.

Table 4: The contaminant removal effectiveness (CRE) of different air distribution systems.

	S1					S2				
	ε_{P1}	ε_{P2}	ε_{P3}	ε_{P4}	ε_{mean}	ε_{P1}	ε_{P2}	ε_{P3}	ε_{P4}	ε_{mean}
O-Low-4x600	0.63	0.99	1.25	0.98	1.07	1.02	0.90	1.25	0.98	1.08
O-Low-2x600	0.88	1.05	1.34	1.01	1.13	1.13	0.77	1.17	1.12	1.14
O-Low-2x1200	0.78	0.98	1.14	1.01	1.04	0.94	0.83	1.10	0.99	1.01
O-Low-1x1200	0.94	1.08	1.24	1.09	1.14	1.04	1.04	1.12	1.01	1.06
O-Medium-4x600	0.69	0.84	1.12	0.94	0.97	1.21	0.37	1.12	1.12	1.15
O-Medium-2x1200	0.86	0.94	1.23	1.09	1.09	1.12	0.89	1.06	1.03	1.07
M-High-4x600	0.18	0.93	0.66	0.89	0.83	1.04	0.95	1.05	0.22	1.01
M-High-2x1200	0.35	1.02	0.89	1.12	1.01	1.07	1.04	1.02	0.27	1.04

Note: Values on a grey background represent the measuring points close to the pollution source. ε_{mean} represents the mean value of CRE of the three measuring points other than the point close to the pollution source.

In addition to the evaluation index for CRE, the heat removal effectiveness (HRE) was also used to characterize the ventilation performance of various strategies. The contours of the HRE in the occupied zone for different air distribution strategies are revealed in Fig. 9. It can be seen that for the low and medium heat gain conditions, more than half of the occupied zone had a value above 1. The active chilled beam systems under low and medium heat gain conditions exhibited slightly higher HRE than the systems under high heat gain conditions. For the O-Low-4x600 case and the O-Low-2x1200 case, the chilled beam ventilation systems provided a uniform thermal environment. But the side close to the mock-up window wall accelerated the cooling of the surrounding air, so

presenting a larger HRE. For the O-Low-2x600 case, with the two chilled beams on the upper left and lower right and the cold convection flow from the mock-up window wall pushing air downwards, air diffused to the lower right locations resulting in a higher HRE. The reasons for the O-Medium-4x600 and O-Medium-2x1200 cases were similar to the O-Low-4x600 and O-Low-2x1200 cases, respectively.

For the M-High-4x600 and M-High-2x1200 cases, the high heat gains and high supply airflow rate contributed to the non-uniform heat characteristics. The HRE varied significantly in different indoor locations and a majority of zones had a value of HRE less than 1. But the frequency of an extremely large HRE increased with increasing heat gain and supply airflow rate. Compared to other cases, the M-High-2x1200 case had the worst heat removal effectiveness.

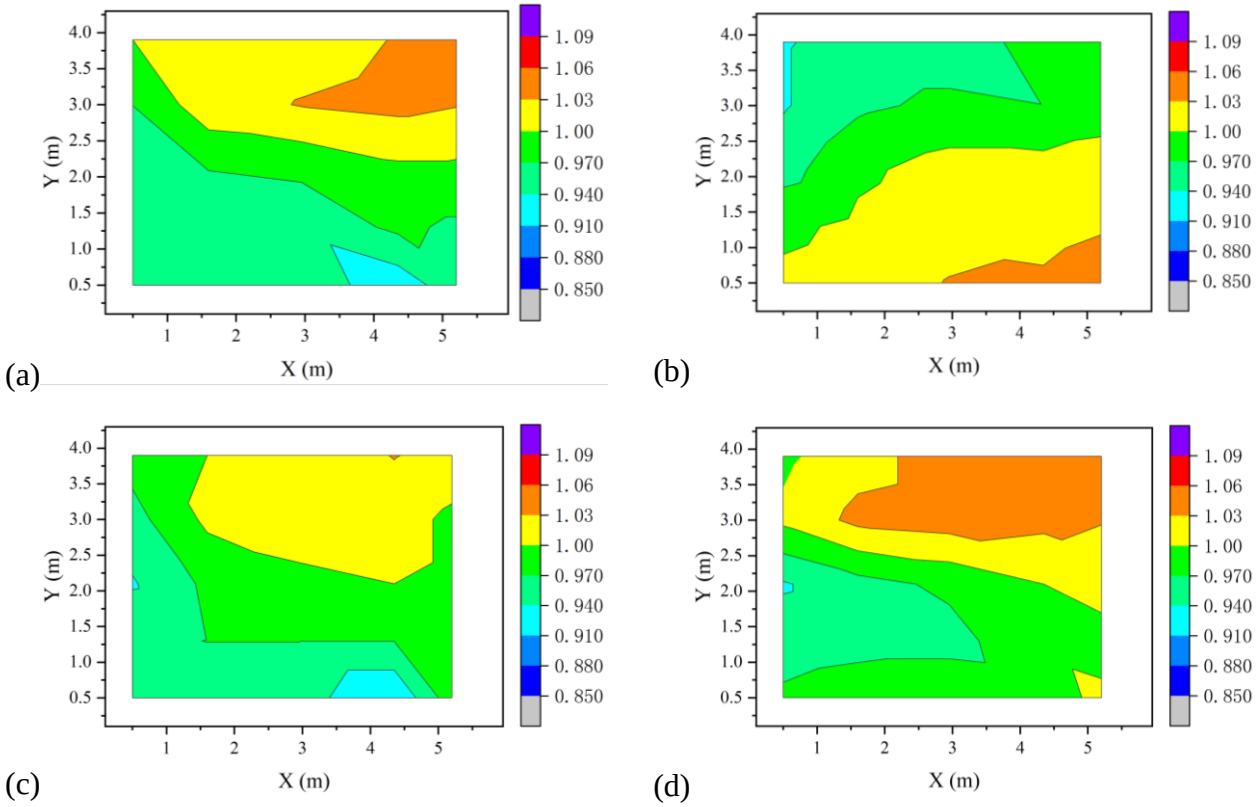

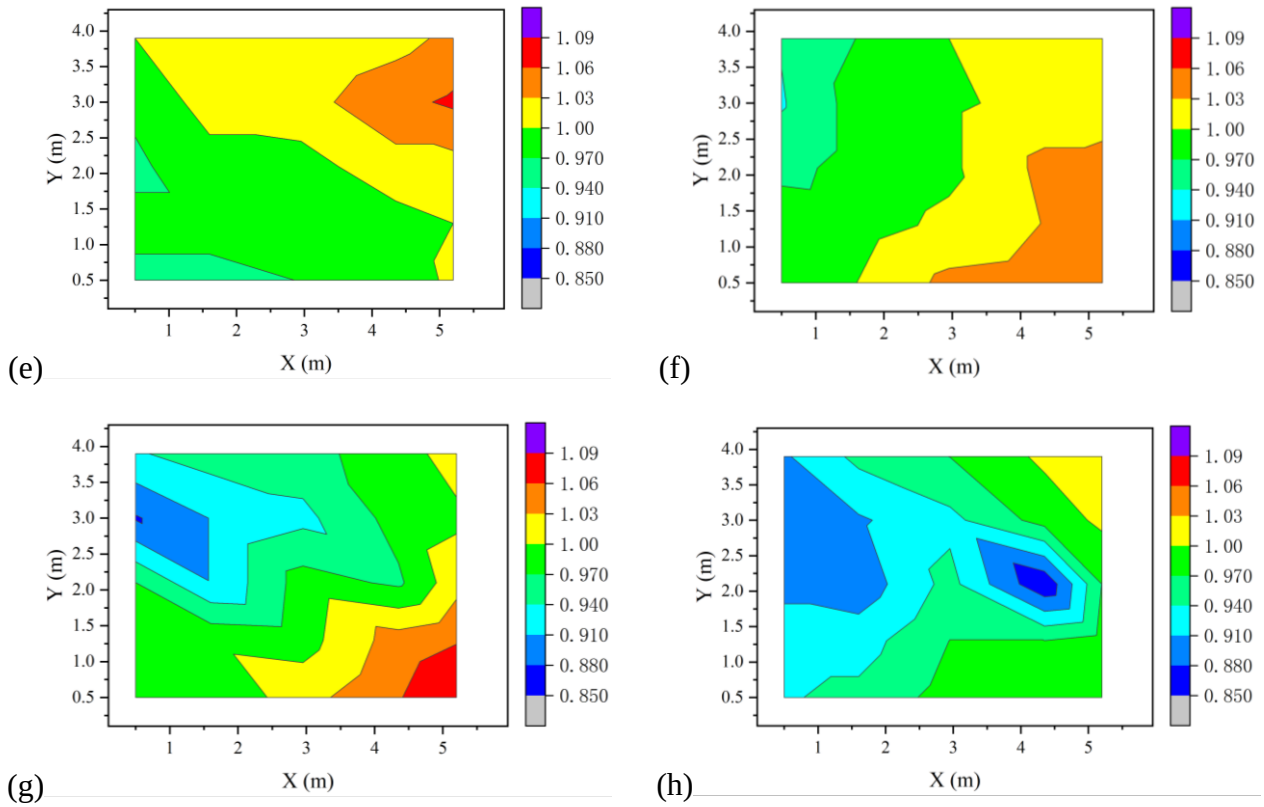

Fig.9: The heat removal effectiveness (HRE) of different air distribution systems: (a) O-Low-4x600 case; (b) O-Low-2x600 case; (c) O-Low-2x1200 case; (d) O-Low-1x1200 case; (e) O-Medium-4x600 case; (f) O-Medium-2x1200 case; (g) M-High-4x600 case; (h) M-High-2x1200 case.

3.4. Thermal comfort analysis

3.4.1. Draught rate (DR)

Fig.10 demonstrates the cumulative distributions of the draught rate (DR) within the occupied zone under the 4-way active chilled beam systems. According to the categories of thermal environments based on ISO 7730, a DR of less than 10% can be classified as Category A and a DR of less than 20% as Category B. It can be seen from Fig.10 that almost all the systems satisfied the requirement of Category B.

As the heat gain increased, there was a decrease in the percentage satisfying the requirement for Category A. For the low heat gain conditions, more than 60% of the points meet the requirement of Category A, and the probability was above 80% in the O-Low-4x600 and O-Low-2x600 cases. The

probability of DR<10% was about 60% and 35% for the medium and high heat gain conditions, respectively. This was because, for the high heat gain conditions, the vertical temperature gradient increased with height, and the room air velocity level was higher.

Under the low heat gain conditions, the 4 pcs and 2 pcs 600 chilled beam systems had similar probability distributions of DR, with more than 80% of the points meeting the Category A standard. The performance of 2 pcs of 1200 chilled beam was better than that of 1 pc of 1200 chilled beam, and the difference in DR between the two cases for meeting Category A was 15%. For all heat gain conditions, the draught performance of 600 chilled beams was better than that of 1200 chilled beams.

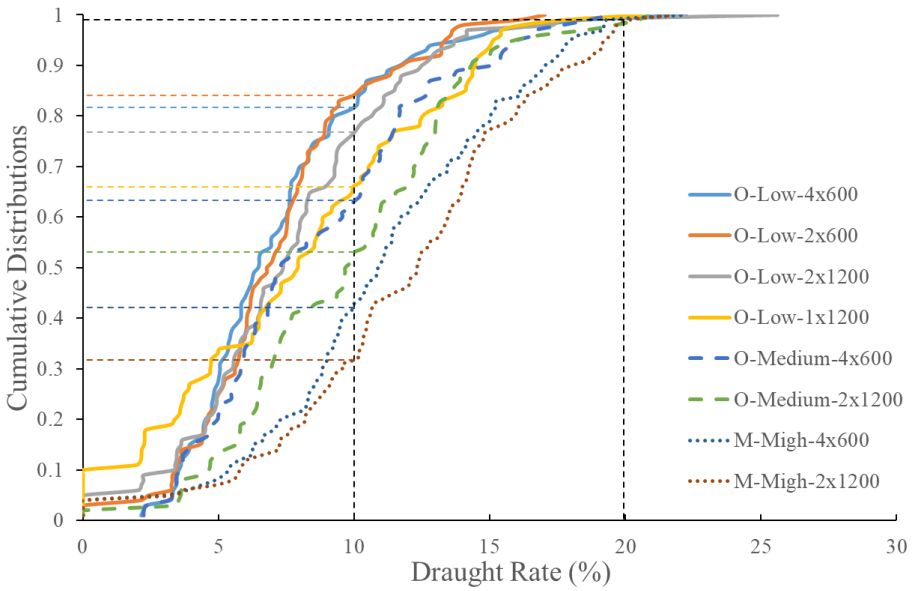

Fig.10: The cumulative distributions of draught rate (DR) in the occupied zone with different chilled beam types.

3.4.2. Air Diffusion Performance Index (ADPI)

The effective draft temperature (EDT) has been a reliable tool to evaluate the thermal comfort of ventilation systems by simultaneously considering the air temperature and velocity [42, 43]. Table 5 illustrates the ranges of effective draft temperature and air diffusion performance index (ADPI) in the

occupied zone under different air distribution systems. An EDT with a smaller deviation can indicate a more uniform thermal environment and it is comfortable for sedentary occupants to sit in a room with an EDT of between -1.5°C and 1.0°C.

As shown in Table 5, the EDT of O-Low-4x600, O-Low-2x600, and O-Low-2x1200 cases were within the acceptable range. With the low heat gain level, a large range of EDT was observed in the O-Low-1x1200 case, caused by the high-speed cold air descending, most noticeably along the left wall. A larger range of EDT denotes that the environment created by the 4-way active chilled beam system under the medium and high heat gain conditions was less comfortable.

In addition to the EDT index, we also evaluated thermal performance using ADPI based on DR<10% and DR<20%, corresponding to Categories A and B for the thermal environment [44, 45]. Studies demonstrate that, in practice, a system that achieves more than 80% of ADPI is considered to be acceptable in terms of air mixture [15, 44]. In terms of ADPI, the active chilled beam system was compliant with Category B in all cases. In fact, the ADPI of both O-Low-4x600 and O-Low-2x600 cases even met Category A. As for the O-Low-1x1200 case, the air velocity distribution and the temperature distribution were very wide because the air jetted along the left wall at high velocity and low temperature. As a result, the ADPI of the O-Low-1x1200 case was estimated to be 56% (with DR<10%) and 88% (with DR<20%). The value of ADPI decreased with increasing heat gain, especially when the DR was less than 10%. In general, with more chilled beams and a more uniform layout, the environment will be more comfortable.

Table 5: The summary of the Air Diffusion Performance Index (ADPI) of different air distribution systems.

	EDT (°C)				ADPI (%)	
	Avg.	Max.	Min.	Std.	With DR<10%	With DR<20%

O-Low-4x600	0.0	0.8	-1.4	0.5	81	99
O-Low-2x600	0.0	0.9	-1.4	0.5	81	97
O-Low-2x1200	0.0	1.0	-1.0	0.4	71	94
O-Low-1x1200	0.0	1.2	-1.7	0.6	56	88
O-Medium-4x600	0.0	0.9	-1.8	0.6	63	98
O-Medium-2x1200	0.0	1.3	-1.3	0.5	50	95
M-High-4x600	0.0	1.8	-1.9	0.7	32	87
M-High-2x1200	0.0	1.7	-1.4	0.6	24	91

4. Discussion

This study shows that the influence of different heat gain levels and different types/layouts of the chilled beams on the thermal comfort and air distributions is varied. Overall, the airflow and temperature patterns created by the 4-way active chilled beam systems produce good thermal conditions in the occupied zone. This supports previous conclusions that chilled beam systems can achieve the twofold goals of providing a comfortable indoor environment and reducing energy consumption [12, 15, 25, 46]. With the outbreak of COVID-19, the WHO's new road map stated that ventilation systems can reduce indoor COVID-19 infections [47], and effective ventilation is considered a key factor in lowering the spread of indoor pollutants [2, 48-50]. Therefore, it is essential to provide a comprehensive evaluation of the 4-way active chilled beam ventilation system under different conditions.

For this purpose, Table 6 illustrates a comprehensive rating scale for the eight cases based on air distribution, heat removal performance, pollutant removal performance, human thermal comfort, and economic cost, with one to five-star asterisks representing the lowest to the highest scoring. By recommending the operating range of different chilled beam systems under variable conditions, valuable practical information for indoor environment creation can be provided at the system design and operation stages.

The system design stage aims to provide the occupants with an appraisal and recommendations to ensure the project is technically and financially feasible. The heat gain levels are initially determined in accordance with the room usage, and then the appropriate number and type of chilled beams is selected according to different indoor heat gain levels. Overall, 2 pcs of 600 chilled beams showed the peak performance under the low heat gain condition, followed by 4 pcs of 600 and 2 pcs of 1200 chilled beams. For the medium heat gain condition, there was no significant difference between the two active chilled beam systems. For the high heat gain condition, 2 pcs of 1200 chilled beam system performed slightly better than the 4 pcs of 600 chilled beam system. At the same time, maximizing the fulfillment of the room occupants' requirements is equally important. For example, when the indoor heat gain level is low and occupants are more concerned about room comfort and pollutant removal efficiency, the 2 pcs of 600 chilled beam system will be the best choice, followed by 4 pcs of 600 and 2 pcs of 1200 chilled beams. If occupants are more concerned about the economic cost and heat removal performance, the 1 pc of 1200 chilled beam system is worth choosing.

Gaining insight into the technical information for the 4-way active chilled beam systems can help drive sustainability at the operation stage. To accommodate the variability in occupants' locations in office and meeting rooms, thermal uniformity is easier to achieve when more units of the chilled beam system are installed. In this regard, 2 and 4 pcs of 600 chilled beam systems are somewhat better than 1 and 2 pcs of 1200 chilled beam systems. Considering that the indoor heat gains increase during the operation stage, the 4 pcs of 600 chilled beam system still performed well in the medium and high heat gain conditions. In a real environment, the internal heat gains characteristic with flexibility. It can be seen from Table 6 that 4 pcs of 600 chilled beam system stand

out in ventilation performance and human thermal comfort when the heat gain level changes. For this consideration, 2 and 4 pcs of 600 chilled beam systems had a better performance in promoting sustainability during the operation stage, especially when the indoor heat gains change flexibly.

Integrating the system design and operation stage, the 2 and 4 pcs of 600 chilled beam systems had a better comprehensive evaluation. However, no consistent conclusions have been reached because of the variability of the requirements. It is proposed to incorporate the concept of flexibility and malleability according to indoor heat load characteristics and occupants' requirements when recommending and selecting a room system for a real case.

Table 6: The comprehensive comparison of the 4-way active chilled beam systems under different conditions.

	Air distribution	Heat removal performance	Pollutant removal performance	Thermal comfort	Economic cost
O-Low-4x600	*****	****	****	*****	*
O-Low-2x600	*****	*****	*****	*****	***
O-Low-2x1200	****	***	****	****	**
O-Low-1x1200	**	*****	*****	***	****
O-Medium-4x600	***	***	***	***	*
O-Medium-2x1200	***	***	****	**	**
M-High-4x600	*	**	*	*	*
M-High-2x1200	*	*	**	*	**

In spite of comprehensively comparing and revealing the thermal and ventilation performance of the 4-way active chilled beam systems under variable heat gain conditions and different types/layouts of the chilled beams, there remain several uncertainties and limitations worthy of further discussion. First, due to the indoor environment involving dynamic conditions, measuring the entire space simultaneously was impossible since the measurement system needed time to stabilize its readings when moving from place to place. Meanwhile, there were small changes in the outside weather and

other environmental parameters over time. Hence, further studies of spatial distribution should take into account the slight time differences during the measurement. Second, the cylindrical dummy without breathing replaced occupants in the room thereby ignoring the effect of occupants' breathing and movement on pollutants and ventilation performance when evaluating the CRE index. Previous studies found that inhalation and deposition in the respiratory system can affect the transmission of pollutants in an air distribution system [51, 52]. Thus, it is recommended that further studies include the effect of inhalation and deposition in the respiratory system when evaluating the ventilation performance of 4-way active chilled beam systems.

5. Conclusions

This study carried out a comprehensive evaluation of thermal comfort and air distribution in a mock-up office and meeting rooms with different terminal layouts of a 4-way active chilled beam ventilation system. The active ventilation system with two/four 600 chilled beams (sized 0.6m x 0.6m) or one/two 1200 chilled beam (sized 1.2m x 0.6m) in different ceiling locations were compared with each other. This comparative experimental study is crucial in providing practical insights into the operating range of active chilled beam systems under variable heat gain and different types/layouts of chilled beams. Results showed the air distribution and local thermal conditions were highly affected by heat load levels and the layouts of active chilled beam terminals. The key findings can be summarized in detail as follows:

(1) With the heat gain increased, the airflow pattern was changed by the increased airflow volume/pressure, resulting in a lower heat removal effectiveness (HRE), the worse the indoor thermal uniformity, the risk of draught increases. The two types of chilled beam can both achieve a

similar mean room air temperature and air velocity. Overall, their air temperature and velocity distribution were acceptable, with slight differences in local thermal comfort and ventilation effectiveness.

(2) In terms of local thermal comfort, the 600 chilled beam systems generally provided higher performance than did the 1200 chilled beam systems. Results showed the local thermal comfort when using 4 pcs 600 chilled beams was generally better than the 2 pcs 1200 chilled beams at the same airflow volume for all low, medium, and high heat gain levels, regarding ADPI (%, DR<10%). In the low heat gain level, the performance of local thermal comfort by using 2 pcs 600 chilled beams was almost as good as the 4 pcs 600 chilled beams, and better than the 1 pc 1200 chilled beam. But ADPI (%, DR<20%) for the 2 pcs 1200 chilled beams was slightly better than the 4 pcs 600 chilled beams under the high heat load conditions.

(3) Generally, the 1200 chilled beam system provided higher performance than the 600 chilled beams regarding heat removal effectiveness (HRE) and contaminant removal effectiveness (CRE). Under high heat gain conditions, the longer type of chilled beam (1200) was more efficient overall than the shorter type (600). When considering the CRE, the performance of the 1200 chilled beams was better than that of the 600 chilled beams. Especially, the O-Medium-4×600 and M-High-4×600 cases displayed poor contaminant removal performance. It is worth noting that pollutant source locations had little impact on CRE, and the chilled beam systems under low heat gain and medium heat gain conditions can remove the pollutants near the source effectively; however, this effect was not obvious under the high heat gain conditions.

The practical recommendations for system design and operation stages are provided based on the operating range of active chilled beam systems under variable heat gain conditions and for

different types/layouts of the units. When the heat load level was not very high, the shorter type of chilled beam is recommended if human thermal comfort is highly desired; selecting the longer type of chilled beam is recommended if the focus is on the indoor air quality. However, under the high heat load conditions, the performance of the 1200 chilled beams is better. Considering the flexibility of heat gain levels during the operation stage, 600 chilled beams are recommended because of the adaptation in ventilation and thermal performance under the changing heat gains. In addition, it is worth mentioning that the findings in this study were based on three specific heat gain levels and four specific terminal layouts. Further studies need to be performed to evaluate the performance under different room geometries, location of heat sources and heat gain levels for the application in various other types and conditions of indoor spaces.

Acknowledgement

This work was supported by Business Finland in Motti Business Finland project (9115/31/2019), the Natural Science Foundation of Chongqing, China [Grant No: cstc2021ycjh-bgzxm0156], and the International Research Centre project [Grant No: B13041]. The author, Ru Ming, would like to thank the Chinese Scholarship Council [No: 201906050234] for their sponsorship of a research study visit to Aalto University in Finland. Specially, the author, Ru Ming would like to thank Weixin Zhao, Minzhou Chen and Tianchen Xue for their mental support during the experimental and data analysis stages.

References

[1] W.H.O. (WHO), WHO Coronavirus (COVID-19) Dashboard. https://covid19.who.int/. (Accessed May 20 2022).

[2] L. Morawska, J. Cao, Airborne transmission of SARS-CoV-2: The world should face the reality, Environment international 139 (2020) 105730.

[3] W. Su, B. Yang, A. Melikov, C. Liang, Y. Lu, F. Wang, A. Li, Z. Lin, X. Li, G. Cao, Infection probability under different air distribution patterns, Building and Environment 207 (2021) 108555.
[4] X. Yang, C. Ou, H. Yang, L. Liu, T. Song, M. Kang, H. Lin, J. Hang, Transmission of pathogen-laden expiratory droplets in a coach bus, Journal of hazardous materials 397 (2020) 122609.
[5] T. Akimoto, S.-i. Tanabe, T. Yanai, M. Sasaki, Thermal comfort and productivity-Evaluation of workplace environment in a task conditioned office, Building and environment 45(1) (2010) 45-50.
[6] S. Lestinen, S. Kilpeläinen, R. Kosonen, J. Jokisalo, H. Koskela, Experimental study on airflow characteristics with asymmetrical heat load distribution and low-momentum diffuse ceiling ventilation, Building and Environment 134 (2018) 168-180.
[7] D. Müller, C. Kandzia, R. Kosonen, A.K. Melikov, P.V. Nielsen, Mixing ventilation: Guide on mixing air distribution design, REHVA: Federation of European Heating and Air-conditioning Associations2013.
[8] P. Wargocki, D.P. Wyon, Ten questions concerning thermal and indoor air quality effects on the performance of office work and schoolwork, Building and Environment 112 (2017) 359-366.
[9] U. Haverinen-Shaughnessy, R.J. Shaughnessy, E.C. Cole, O. Toyinbo, D.J. Moschandreas, An assessment of indoor environmental quality in schools and its association with health and performance, Building and Environment 93 (2015) 35-40.
[10] H. Latif, G. Hultmark, S. Rahnama, A. Maccarini, A. Afshari, Performance evaluation of active chilled beam systems for office buildings–A literature review, Sustainable Energy Technologies and Assessments 52 (2022) 101999.
[11] D. Alexander, M. O'Rourke, Design considerations for active chilled beams, ASHRAE Journal 50(9) (2008) 50-58.
[12] A.S. Azad, D. Rakshit, M.P. Wan, S. Babu, J.N. Sarvaiya, D.K. Kumar, Z. Zhang, A.S. Lamano, K. Krishnasayee, C.P. Gao, Evaluation of thermal comfort criteria of an active chilled beam system in tropical climate: A comparative study, Building and Environment 145 (2018) 196-212.
[13] S. Riffat, X. Zhao, P. Doherty, Review of research into and application of chilled ceilings and displacement ventilation systems in Europe, International Journal of Energy Research 28(3) (2004) 257-286.
[14] B. Wu, W. Cai, H. Chen, K. Ji, Experimental investigation on airflow pattern for active chilled beam system, Energy and Buildings 166 (2018) 438-449.
[15] K.-N. Rhee, M.-S. Shin, S.-H. Choi, Thermal uniformity in an open plan room with an active chilled beam system and conventional air distribution systems, Energy and Buildings 93 (2015) 236-248.
[16] P. Mustakallio, Z. Bolashikov, K. Kostov, A. Melikov, R. Kosonen, Thermal environment in simulated offices with convective and radiant cooling systems under cooling (summer) mode of operation, Building and Environment 100 (2016) 82-91.
[17] R. Kosonen, P. Mustakallio, A. Melikov, M. Duszyk, Comparison of the thermal environment in rooms with chilled beam and radiant panel systems, Proceedings of Roomvent conference. Trondheim, 2011.
[18] G. Cao, M. Sivukari, J. Kurnitski, M. Ruponen, O. Seppänen, Particle Image Velocimetry (PIV) application in the measurement of indoor air distribution by an active chilled beam, Building and Environment 45(9) (2010) 1932-1940.
[19] J. Fredriksson, M. Sandberg, B. Moshfegh, Experimental investigation of the velocity field and airflow pattern generated by cooling ceiling beams, Building and environment 36(7) (2001) 891-899.
[20] H. Koskela, H. Häggblom, R. Kosonen, M. Ruponen, Flow pattern and thermal comfort in office environment with active chilled beams, HVAC&R Research 18(4) (2012) 723-736.
[21] R. Kosonen, J. Penttinen, The effect of free cooling and demand-based ventilation on energy consumption of self-regulating and traditional chilled beam systems in cold climate, Indoor and Built Environment 26(2) (2017)

256-271.
[22] M. Ruponen, H. Itkonen, P. Mustakallio, J. Jokisalo, Energy savings with very high temperature cooling water active chilled beam system, CLIMA 2010 Conference, WellBeing Indoors, Antalya, Turkey, May 9-12, 2010, 2010, p. 6.
[23] H.M. Sachs, W. Lin, A.K. Lowenberger, Emerging energy saving-HVAC technologies and practices for the buildings sector (2009), American Council for an Energy-Efficient Economy, 2009.
[24] J. Stein, S. Taylor, VAV reheat versus active chilled beams and DOAS, (2013).
[25] M. Cehlin, T. Karimipanah, U. Larsson, A. Ameen, Comparing thermal comfort and air quality performance of two active chilled beam systems in an open-plan office, Journal of Building Engineering 22 (2019) 56-65.
[26] K. Khankari, Comparative Analysis of Overhead Air Supply and Active Chilled Beam HVAC Systems for Patient Room, Chicago: ASHRAE Winter Conference, 2015.
[27] C. Chen, W. Cai, Y. Wang, C. Lin, Further study on the heat exchanger circuitry arrangement for an active chilled beam terminal unit, Energy and Buildings 103 (2015) 352-364.
[28] D. Nam, Z. Zhai, Experimental study on energy performance of active chilled beam systems, Science and Technology for the Built Environment 25(10) (2019) 1369-1379.
[29] P. Filipsson, A. Trüschel, J. Gräslund, J.-O. Dalenbäck, Induction ratio of active chilled beams– Measurement methods and influencing parameters, Energy and Buildings 129 (2016) 445-451.
[30] R. Upadhyay, R. Mora, M.-A. Jean, M. Koupriyanov, Experimental study on the performance evaluation of active chilled beams in heating and cooling operation under varied boundary conditions, Science and Technology for the Built Environment 26(5) (2020) 658-675.
[31] B. Wu, W. Cai, K. Ji, Heat source effects on thermal comfort for active chilled beam systems, Building and Environment 141 (2018) 91-102.
[32] A.K. Melikov, B. Yordanova, L. Bozkhov, R. Kosonen, Airflow distribution in rooms with active chilled beams, 2007.
[33] R. Kosonen, A. Melikov, B. Yordanova, L. Bozkhov, Impact of heat load distribution and strength on airflow pattern in rooms with exposed chilled beams, Proceedings of ROOMVENT, 2007, pp. 10-14.
[34] B. Wu, Air distribution and thermal comfort for active chilled beam systems, Nanyang Technological University, 2018.
[35] M. Mundt, H. Mathisen, M. Moser, P. Nielsen, REHVA Ventilation Effectiveness Guide, Federation of European Heating, Ventilation and Air-Conditioning Association 2004.
[36] B. Olesen, M. Scholer, P. Fanger, Discomfort caused by vertical air temperature differences, Indoor climate 36 (1979) 561-578.
[37] R. Ilmarinen, J. Palonen, O. Seppänen, Effects of non-uniform thermal conditions on body temperature responses in women, Proceedings of the 41st Nordiska Arbetsmiljömötet (1992) 181-182.
[38] L. Schellen, M.G. Loomans, M.H. de Wit, B.W. Olesen, W. van Marken Lichtenbelt, The influence of local effects on thermal sensation under non-uniform environmental conditions—Gender differences in thermophysiology, thermal comfort and productivity during convective and radiant cooling, Physiology & behavior 107(2) (2012) 252-261.
[39] A. Ashrae, Standard 55-2013: Thermal Environmental Conditions for Human Occupancy, American Society of Heating, Refrigerating, and Air-Conditioning Engineers, Inc. Atlanta (2013).
[40] P.O. FANGER, N. Christensen, Perception of draught in ventilated spaces, Ergonomics 29(2) (1986) 215-235.
[41] W.K. Chow, L.T. Wong, Experimental studies on air diffusion of a linear diffuser and associated thermal comfort indices in an air-conditioned space, Building and Environment 29(4) (1994) 523-530.

[42] Z. Lin, Effective draft temperature for evaluating the performance of stratum ventilation, Building and environment 46(9) (2011) 1843-1850.
[43] X. Kong, C. Xi, H. Li, Z. Lin, A comparative experimental study on the performance of mixing ventilation and stratum ventilation for space heating, Building and Environment 157 (2019) 34-46.
[44] D.A. John, Designing air-distribution systems to maximize comfort, ASHRAE Journal 54(9) (2012) 20-25.
[45] D.J. Thevenard, R.G. Humphries, The Calculation of Climatic Design Conditions in the 2005 ASHRAE Handbook--Fundamentals, ASHRAE Transactions 111(1) (2005).
[46] Z. Shi, Z. Lu, Q. Chen, Indoor airflow and contaminant transport in a room with coupled displacement ventilation and passive-chilled-beam systems, Building and Environment 161 (2019) 106244.
[47] W.H. Organization, Roadmap to improve and ensure good indoor ventilation in the context of COVID-19, (2021).
[48] L. Morawska, J.W. Tang, W. Bahnfleth, P.M. Bluyssen, A. Boerstra, G. Buonanno, J. Cao, S. Dancer, A. Floto, F. Franchimon, How can airborne transmission of COVID-19 indoors be minimised?, Environment international 142 (2020) 105832.
[49] J.-X. Wang, X. Cao, Y.-P. Chen, An air distribution optimization of hospital wards for minimizing cross-infection, Journal of Cleaner Production 279 (2021) 123431.
[50] H. Qian, X. Zheng, Ventilation control for airborne transmission of human exhaled bio-aerosols in buildings, Journal of thoracic disease 10(Suppl 19) (2018) S2295.
[51] F. Liu, Z. Luo, Y. Li, X. Zheng, C. Zhang, H. Qian, Revisiting physical distancing threshold in indoor environment using infection-risk-based modeling, Environment international 153 (2021) 106542.
[52] B.C. Singer, H. Zhao, C.V. Preble, W.W. Delp, J. Pantelic, M.D. Sohn, T.W. Kirchstetter, Measured influence of overhead HVAC on exposure to airborne contaminants from simulated speaking in a meeting and a classroom, Indoor air (2021).